Obrabotka metallov (tekhnologiya, oborudovanie, instrumenty) = Metal Working and Material Science. 2022 vol. 24 no. 4 pp. 181–191
ISSN: 1994-6309 (print) / 2541-819X (online)
DOI: 10.17212/1994-6309-2022-24.4-181-191

NSTU NETI

Obrabotka metallov - Metal Working and Material Science

Journal homepage: http://journals.nstu.ru/obrabotka_metallov

Residual stress estimation in crystalline phases of high-entropy alloys of the $Al_xCoCrFeNi$ system

Ivan Ivanov [1, a, *], *Aleksandr Yurgin* [1, b], *Igor Nasennik* [1, c], *Konstantin Kuper* [2, 3, d]

[1] Novosibirsk State Technical University, 20 Prospekt K. Marksa, Novosibirsk, 630073, Russian Federation
[2] Budker Institute of Nuclear Physics of the Siberian Branch of the RAS, 11, Ac. Lavrentieva ave., Novosibirsk, 630090, Russian Federation
[3] Federal Research Center Boreskov Institute of Catalysis, 11, Ac. Nicolskiy ave., Koltsovo, 630559, Russian Federation

[a] https://orcid.org/0000-0001-5021-0098, i.ivanov@corp.nstu.ru, [b] https://orcid.org/0000-0003-0473-7627, yurgin2012@yandex.ru,
[c] https://orcid.org/0000-0003-0937-5004, goga.mer@mail.ru, [d] https://orcid.org/0000-0001-5017-6248, k.e.kuper@inp.nsk.su

ARTICLE INFO

Article history:
Received: 13 September 2022
Revised: 26 September 2022
Accepted: 06 October 2022
Available online: 15 December 2022

Keywords:
High-entropy alloys
AlxCoCrFeNi
Plastic deformation
Residual stresses
Synchrotron X-ray diffraction

Funding
This study was funded according to Russian Science Foundation research project № 20-73-10215 “In-situ study of the evolution of the dislocation structure of plastically deformed high-entropy alloys under high-pressures and temperatures using synchrotron radiation”. Research was conducted at core facility “Structure, mechanical and physical properties of materials”.

ABSTRACT

Introduction. All plastically deformed alloys are characterized by crystal defects that increase the internal energy of the system. These defects also result in residual stresses that have a complex effect on the material properties. Macrostresses are often the most critical and can lead to warpage, reduced corrosion resistance, and changes in material strength characteristics. **The purpose of this work is to** assess the residual stresses of the primitive cubic phase of high entropy alloys $Al_{0.6}CoCrFeNi$ and *AlCoCrFeNi*. **Research methods**. The crystal structure of the alloys is studied using the method of X-ray diffraction analysis. Experiments on X-ray diffraction analysis were carried out at the Siberian Center for Synchrotron and Terahertz Radiation on a *VEPP-4* (Novosibirsk, INF SB RAS, 5-A line «X-ray microscopy and tomography»). Studies using synchrotron radiation were carried out in the transmission mode. The evaluation of the residual macrostresses of the crystalline phases of the alloys was based on the analysis of the change in the shape of the diffraction rings with a change in the azimuth angle (χ). **Materials**. The objects of research are ingots of high-entropy alloys $Al_{0.6}CoCrFeNi$ and *AlCoCrFeNi*. The ingots were obtained from pure metals by argon arc melting with cooling on a copper plate. To conduct further studies, cylindrical samples are cut from the ingots, which were subjected to plastic deformation according to the uniaxial compression scheme. **Results and discussion**. The obtained results indicate that the $Al_{0.6}CoCrFeNi$ alloy is characterized by higher macrostresses than the *AlCoCrFeNi* alloy. The residual deformation of the *B2* phase lattice of *AlCoCrFeNi* alloy along the direction [100] is 2.5% at an external load of 2,500 MPa. The distortion value of the lattice of this phase for the alloy $Al_{0.6}CoCrFeNi$ is equal to 5.5% under similar external conditions. In addition, the plastic deformation of the $Al_{0.6}CoCrFeNi$ *HEA* did not lead to its destruction. This allows concluding that the increased ductility of this alloy is associated not only with the presence of a phase with a *FCC* lattice, but also with an increased compliance of the phase with a primitive lattice.

For citation: Ivanov I.V., Yurgin A.B., Nasennik I.E. Kuper K.E. Residual stress estimation in crystalline phases of high-entropy alloys of the $Al_xCoCrFeNi$ system. *Obrabotka metallov (tekhnologiya, oborudovanie, instrumenty) = Metal Working and Material Science*, 2022, vol. 24, no. 4, pp. 181–191. DOI: 10.17212/1994-6309-2022-24.4-181-191. (In Russian).

Introduction

High entropy alloys (*HEA*s) are a new and one of the most promising classes of materials [1–6]. Due to its structure, *HEA* have high mechanical and physical properties, which make it promising materials for various fields.

*** Corresponding author**
Ivanov Ivan V., Ph.D. (Engineering)
Novosibirsk State Technical University,
20 Prospekt K. Marksa,
630073, Novosibirsk, Russian Federation
Tel.: 8 (383) 346-11-71, **e-mail:** i.ivanov@corp.nstu.ru

High expectations of the *HEA*s applicability are due to its high phase stability [7, 8]. It is known that *HEA* is characterized by the formation of phases with cubic crystal lattices [9, 10]. It was believed that the arrangement of atoms in the *HEA* structure is completely random, which should have determined its high mechanical and physical properties. However, recent studies have shown that *HEA*s contain additional phases, which are characterized by a regular, but not random, arrangement of atoms in the structure [11, 12, 13, 14]. These phases often appear in the *HEA* structure during prolonged thermal exposure [15, 16]. For example, it is known that in some alloys of the $Al_xCoCrFeNi$ system the *B2* and $L1_2$ phases with primitive cubic lattice can be formed [17, 18, 19]. The $Al_xCoCrFeNi$ system is the most promising among all high-entropy alloys due to the possibility of the phase composition flexible control by changing the aluminum content.

The study of strain-stress and thermal-stress states within workpieces obtained from high-entropy alloys is very important from the point of view of the application of these alloys. It is well known that the energy of plastic deformation is accumulated in the structure of metal alloys as the residual stresses. There are three types of internal stresses: macrostresses; microstresses and static lattice distortions [20]. These stresses have a significant effect on the properties of the material. The using of *HEA*s as structural and functional materials requires scientists and engineers to understand the evolution of internal stresses within the crystalline phases of alloys. However, now in the literature there are no studies of residual stresses and residual lattice distortions of high-entropy alloys.

The purpose of this work was to evaluate the residual lattice distortions of the phases of the *AlxCoCrFeNi* alloys after cold plastic deformation. The plastic deformation of $Al_{0.6}CoCrFeNi$ and *AlCoCrFeNi* alloys was carried out by using the axial compression scheme. The calculation of residual lattice distortions was based on synchrotron X-ray diffraction data. The results of this work allow drawing conclusions about the mechanical properties of the phases of high-entropy alloys.

Methods and Materials

In this work, the objects of research were ingots of $Al_{0.6}CoCrFeNi$ and *AlCoCrFeNi* high-entropy alloys. The ingots were obtained from pure metals by using argon-arc melting and cooling on a copper substrate. The shape of the ingots was close to cylindrical. The height of the obtained ingots was about 10 mm. The diameter was about 20 mm. For the most uniform distribution of chemical elements, remelting was carried out at least 10 times. Weight loss during smelting did not exceed 0.2 %. The elemental composition of the ingots was evaluated by X-ray microanalysis using a scanning electron microscope *Carl Zeiss EVO50 XVP* and *Oxford Instruments X-Act* detector. The final value of the elemental composition was determined by averaging from at least twenty different regions of the ingot. The deviation of the composition from the nominal did not exceed 0.6 %.

For further studies, cylindrical samples with a height of 8 mm and a diameter of 5 mm were cut from the ingots. The resulting cylinders were deformed according to the uniaxial compression scheme on a *Instron 3369* machine. At a maximum applied stress of ~2,500 MPa, the deformation of the *AlCoCrFeNi* was 30 % and the deformation of the $Al_{0.6}CoCrFeNi$ was 53 %. Based on these values, the following compression degrees were chosen: 25; 34; 45; 50 and 53 % for the $Al_{0.6}CoCrFeNi$ and 12; 18 and 30 % for *AlCoCrFeNi*.

Metallographic studies of the samples were carried out by the optical microscopy using a *Carl Zeiss Axio Observer* microscope. Before metallographic studies, the samples were subjected to etching with a solution consisting of a copper (II) sulfate, hydrochloric acid, and water (5 ml each).

The crystal structure of the alloys was studied using the X-ray diffraction analysis. *XRD* experiments were carried out in a transmission mode at the beamline *5-A* (X-ray microscopy and tomography) at *VEPP-4* synchrotron source (Budker's Institute of Nuclear Physics, Novosibirsk, Russia). The X-ray wavelength was 0.022 nm. A *mar345s* image plate 2D detector with pixel size 100 × 100 mkm^2 and scan area diameter 345 mm was used to record the diffraction patterns. During the experiments, two-dimensional diffraction patterns were obtained. These two-dimensional diffraction patterns were azimuthally integrated [21].

Results and discussion

The changing of aluminum content in $Al_xCoCrFeNi$ alloys system makes it possible to control the phase composition of materials. Well known, that difference of the phase composition has a significant effect on the mechanical properties of the alloys. Figure 1 shows the compression curves of the studied alloys. The $Al_{0.6}CoCrFeNi$ alloy has a higher ductility compared to the *AlCoCrFeNi* alloy. At the maximum applied stress of ~2,500 MPa, the deformation of the *AlCoCrFeNi* alloy was 30 %, and the deformation of the $Al_{0.6}CoCrFeNi$ alloy was 53 %.

According to the optical metallography results, the structure of the alloys also underwent significant changes after plastic deformation (Figure 2). In both cases, a change in the shape of the grains is observed. Furthermore, the plastic deformation of the $Al_{0.6}CoCrFeNi$ alloy with a compression ratio of 53 % (Figure 2d) does not lead to appearance of cracks. However, in the case of the *AlCoCrFeNi* alloy (Figure 2, *c*), fracture traces appear even after compression by 12 %.

Well known that residual stresses are balanced in different volumes of the deformed body and affect to the position and shape of the diffraction peaks. Macrostresses are balanced in the macro-volumes of the material and lead to a change of the positions of the diffraction maxima and the shape of the diffraction rings. Microstresses are balanced within several crystallites or blocks and lead to a change in the shape (width) of the diffraction peaks. Static stresses are balanced within groups of atoms and lead to an increase of diffuse scattering and, accordingly, an increase of the background intensity. In terms of the mechanical properties of the designed product, macrostresses are the most important since it can lead to warpage.

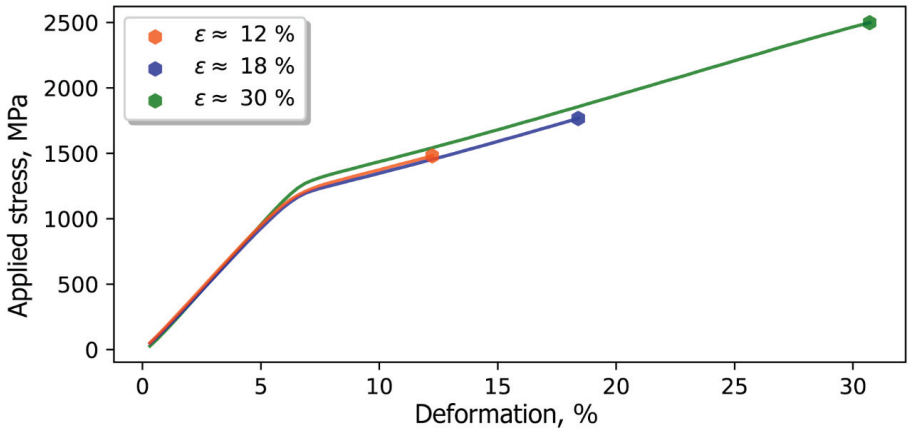

a

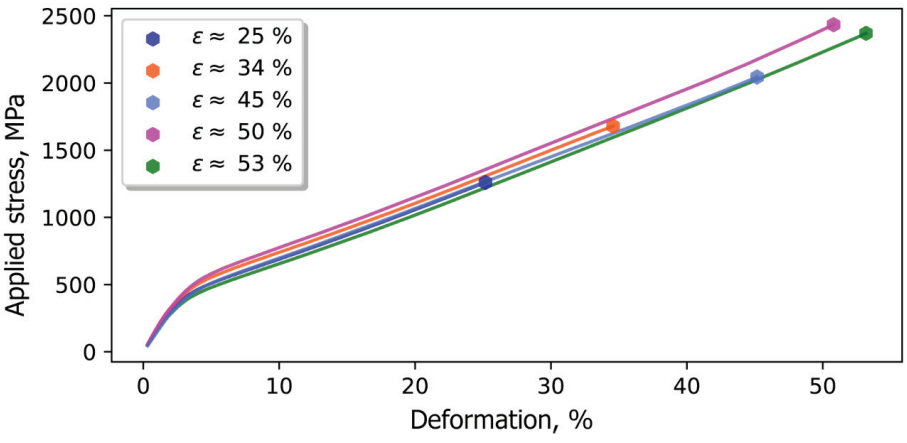

b

Fig. 1. Compression curves of *AlCoCrFeNi* (*a*) и $Al_{0.6}CoCrFeNi$ (*b*) alloys

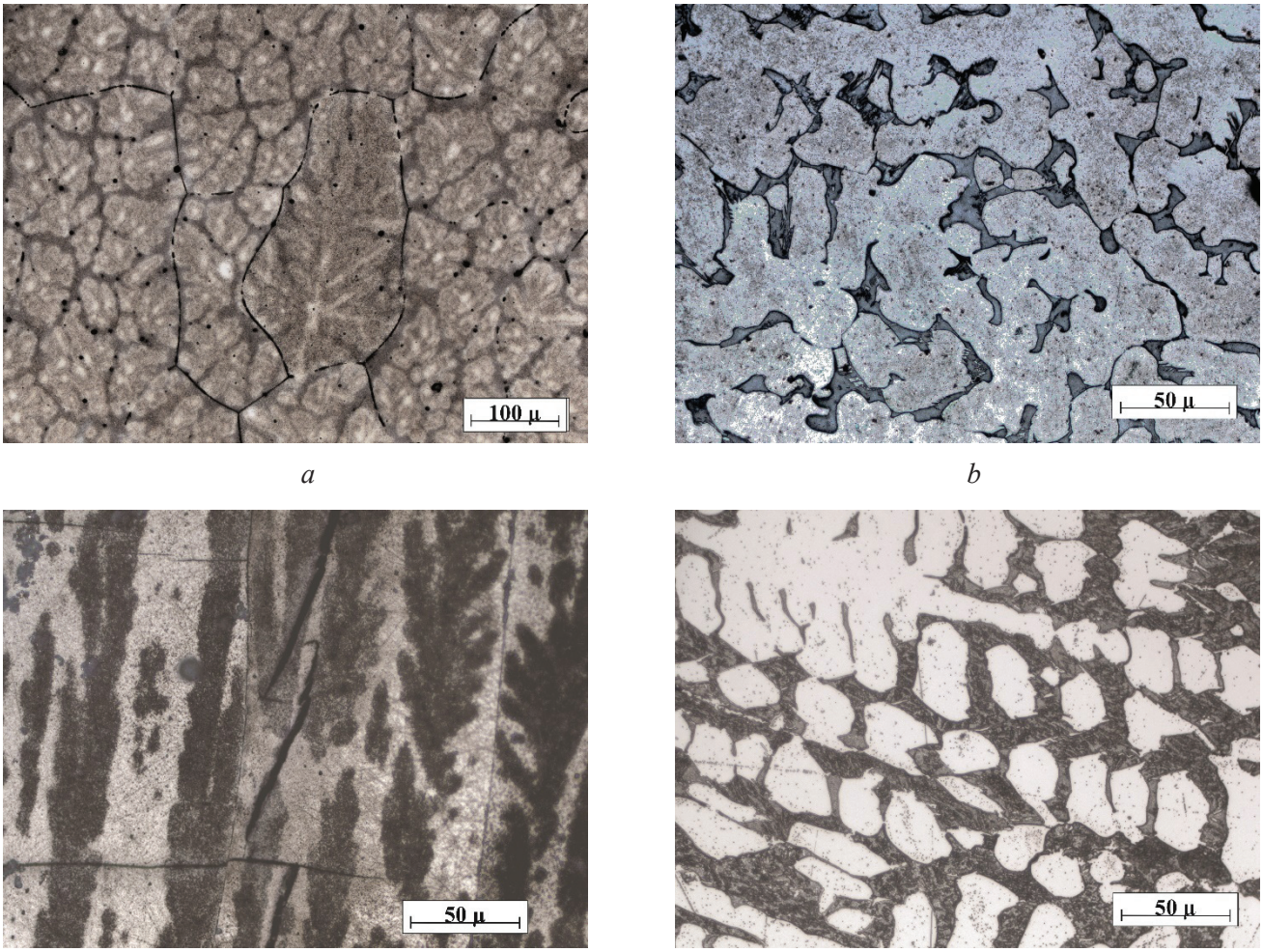

a *b*

c *d*

Fig. 2. Results of metallographic studies: *AlCoCrFeNi* alloy before deformation (*a*), deformed by 12% (*c*); $Al_{0.6}CoCrFeNi$ alloy before deformation (*b*) after 53% compression (*d*)

Estimation of residual macrostresses of crystalline phases of alloys *AlCoCrFeNi* and $Al_{0.6}CoCrFeNi$ was based on the analysis of changes in the shape of diffraction rings with a change in the azimuth angle (χ). In other words, the lattice parameter was estimated for each angle χ. However, in this case, the positions of the diffraction maxima should be clearly distinguishable. Figure 3 shows an example of one-dimensional diffraction patterns obtained in this work.

According to [11, 12], the composition of the *AlCoCrFeNi* alloy includes two phases characterized by cubic crystal system: disordered phase (space group $Im\bar{3}m$) and ordered phase (space group $Pm\bar{3}m$, or *B2* type in *Strukturbericht* terms). Since the lattice parameters of these phases are identical, the diffraction maxima have the same angular positions. Therefore, the analysis of lattice distortions of the *AlCoCrFeNi* alloy is possible only for phase peaks with a primitive lattice. In this work, the calculation was carried out using three diffraction maxima of $Pm\bar{3}m$ phase: (100); (111) and (210). The overlap of the diffraction peaks of $Im\bar{3}m$ and $Pm\bar{3}m$ phases is also typical for the diffraction pattern of the $Al_{0.6}CoCrFeNi$ alloy. At the same time, this alloy also includes a phase with the space group $Fm\bar{3}m$. Therefore, the analysis of the lattice distortions of the primitive cubic phase was carried out only by the diffraction maximum (100) for $Al_{0.6}CoCrFeNi$ alloy.

The analysis of residual macrostresses was carried out according to the obtained 2D diffraction patterns. The diffraction pattern was represented as a scanning in the coordinates "2θ — χ" (Figure 4).

This type of diffraction pattern makes it possible to estimate the lattice distortions by the position of the diffraction maxima along the angle χ. For this, the approximation of the diffraction band by a periodic function is optimal.

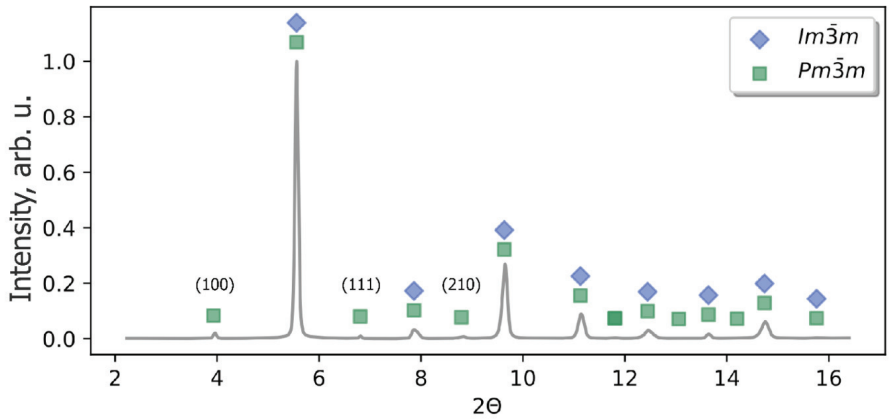

a

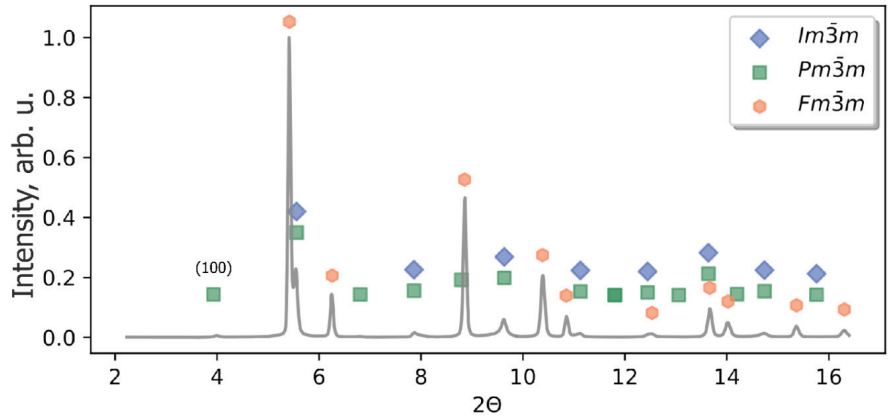

b

Fig. 3. Diffraction patterns of *AlCoCrFeNi* (*a*) and $Al_{0.6}CoCrFeNi$ (*b*) alloys subjected to uniaxial compression by 18 and 25 % respectively

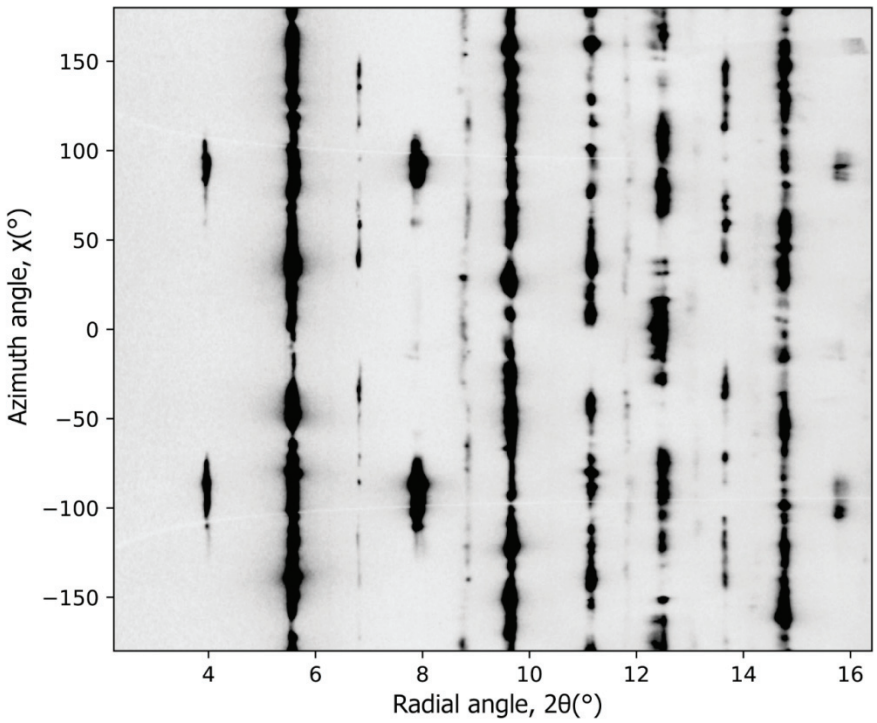

Fig. 4. Scanning of a two-dimensional diffraction pattern of the *AlCoCrFeNi* alloy after uniaxial compression by 18 %

Figure 5 shows examples of scans for three diffraction maxima of the *B2* phase. It follows that the presence of a crystallographic texture leads to the presence of texture maxima for the diffraction peaks (100) and (111). This fact makes it impossible to approximate the diffraction band by a function. Therefore, the analysis of residual stresses was carried out by analyzing the deviation of the average value of the intensity of the diffraction maximum from its zero-position (at the absence of internal stresses).

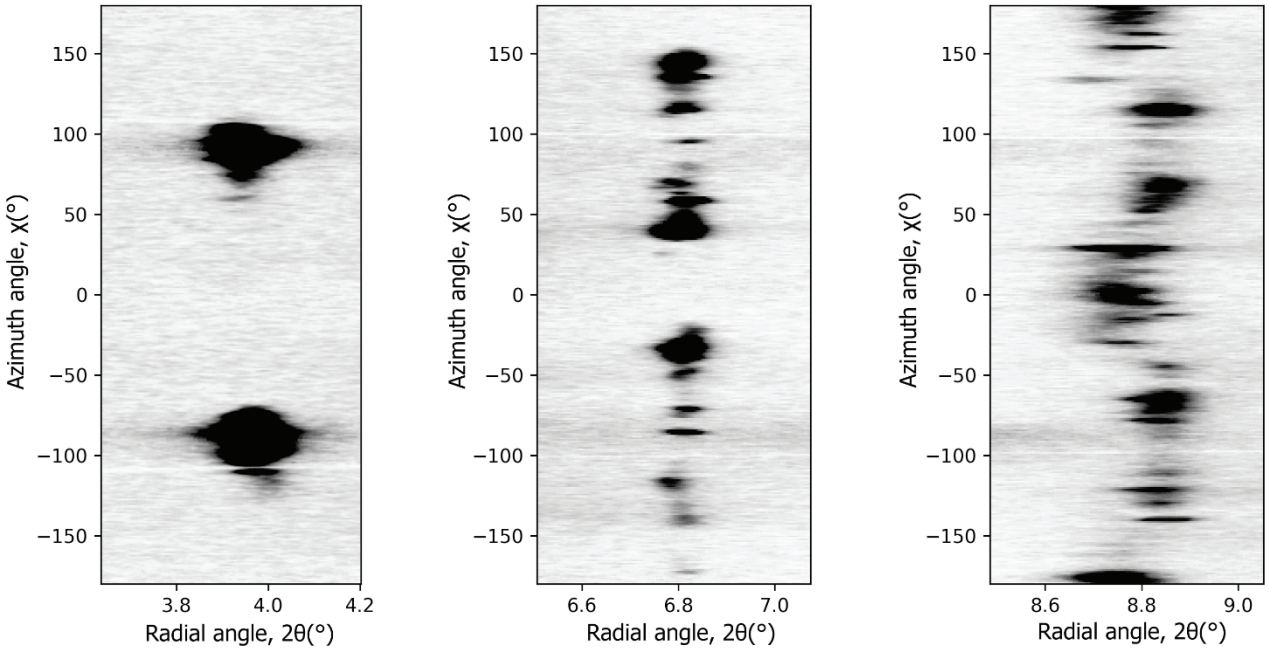

a *b* *c*

Fig. 5. Diffraction maxima (100) (*a*), (111) (*b*) and (210) (*c*) in the coordinates «χ – 2θ» of *B2* phase after uniaxial compression of alloy *AlCoCrFeNi* by 18 %

Figure 6, *a* shows the dependence of the residual lattice distortions on the applied stresses. The largest increase in stresses occurs along the [100] direction. This is due to the anisotropy of the crystal lattice of the *B2* phase. At an applied stress of ~2,500 MPa, the residual distortion of the lattice along this direction was 2.25 %. In addition, the sample before deformation (i.e., in the cast state) is also characterized by the presence of lattice distortions, which is associated with the presence of thermal stresses during cooling of the ingot.

An analysis of the $Al_{0.6}CoCrFeNi$ alloy showed that the *B2* phase of this sample is characterized by a more significant lattice distortion. According to the obtained results (Figure 6, *b*), the lattice distortion under an applied stress ~2,500 MPa was 5.5 %. This fact is in good agreement with the results of optical metallography (Figure 2). Since no cracks or other traces of destruction were found in the structure of the $Al_{0.6}CoCrFeNi$ alloy (Figure 2, *c*), it can be concluded that the structure did not relax due to its destruction. At the same time, the presence of cracks in the structure of the *AlCoCrFeNi* alloy (Figure 2, *d*) indicates to its partial relaxation. This is indicated by the values of crystal lattice distortions (Figure 6, *b*).

The analysis of the deformation of the crystal lattice also makes it possible to estimate the values of the elastic modulus of alloys. However, since the energy of plastic deformation is stored in the structure as both macro- and microstresses, the analysis of the change of the positions of diffraction peaks makes it possible to estimate only the upper limit of possible values of the elastic modulus. However, even such estimate makes it possible to qualitatively compare the properties of the phases of the alloys. According to the obtained results, the maximum value of the elastic modulus of *B2* phase of the *AlCoCrFeNi* alloy along the [100] direction is 111 GPa. At the same time, the maximum value of elastic modulus for the *B2* phase of $Al_{0.6}CoCrFeNi$ alloy along the same direction is equal to 46 GPa. Thus, the lattice of the *B2* phase in the *AlCoCrFeNi* alloy is significantly less compliant than the lattice of the same phase in the $Al_{0.6}CoCrFeNi$ alloy.

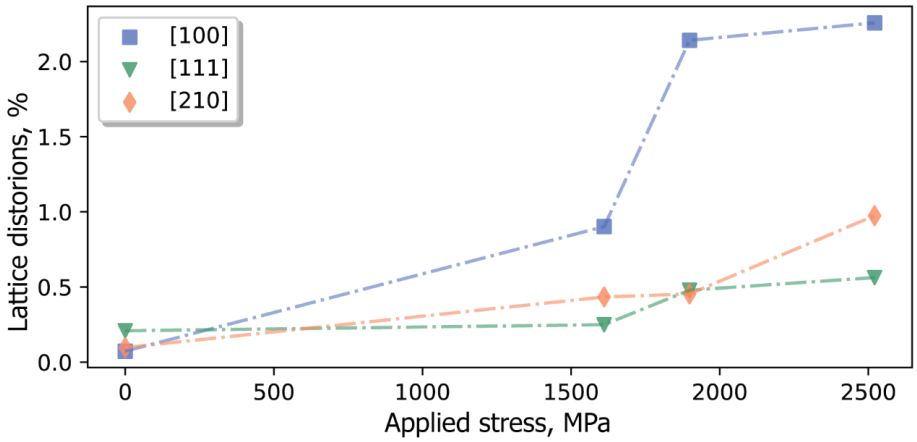

a

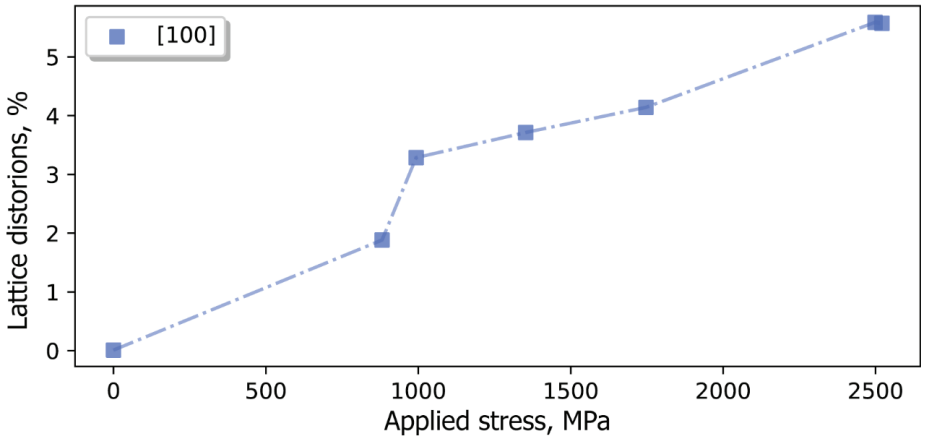

b

Fig. 6. Dependence of the deformation of the *B2* lattice of *AlCoCrFeNi* (*a*) and $Al_{0.6}CoCrFeNi$ (*b*) alloys in the directions [*hkl*] depending on the applied stresses during deformation

Conclusions

1. Plastic deformation of $Al_{0.6}CoCrFeNi$ and *AlCoCrFeNi* alloys leads to significant changes in its structure. The change in grain shape is presented in both materials structure. However, traces of partial fracture are observed only in the case of the *AlCoCrFeNi* alloy. This fact indicates a higher plasticity of the $Al_{0.6}CoCrFeNi$ alloy.

2. Plastic deformation of both alloys leads to significant changes in the shape and positions of the diffraction maxima of the alloys. However, due to the overlap of diffraction maxima, macrostress estimation is possible only for a primitive cubic phase.

3. According to the analysis of the change of diffraction maxima positions, the residual lattice distortions of the *B2* phase along the [100] direction in *AlCoCrFeNi* alloy is 2.5 % at an external load of 2,500 MPa. At the same time, the value of the lattice distortion of the same phase for the $Al_{0.6}CoCrFeNi$ alloy is 5.5 %. This fact indicates the presence of high residual stresses in the structure of the *B2* phase of the $Al_{0.6}CoCrFeNi$ alloy.

4. The obtained results indicate that the high plasticity of the $Al_{0.6}CoCrFeNi$ alloy is associated not only with the presence of the fcc phase, but also with the high compliance of the primitive cubic lattice.

References

1. Bataeva Z.B., Ruktuev A.A., Ivanov I.V., Yurgin A.B., Bataev I.A. Obzor issledovanii splavov, razrabotannykh na osnove entropiinogo podkhoda [Review of alloys developed using the entropy approach]. *Obrabotka metallov (tekhnologiya, oborudovanie, instrumenty) = Metal Working and Material Science*, 2021, vol. 23, no. 2, pp. 116–146. DOI: 10.17212/1994-6309-2021-23.2-116-146.

2. Li X., Schönecker S., Li W., Varga L.K., Irving D.L., Vitos L. Tensile and shear loading of four fcc high-entropy alloys: a first-principles study. *Physical Review B*, 2018, vol. 97 (9), pp. 1–9. DOI: 10.1103/PhysRevB.97.094102.

3. Gorban' V.F., Krapivka N.A., Firstov S.A. Vysokoentropiinye splavy – elektronnaya kontsentratsiya – fazovyi sostav – parametr reshetki – svoistva [High-entropy alloys: interrelations between electron concentration, phase composition, lattice parameter, and properties]. *Fizika metallov i metallovedenie = Physics of Metals and Metallography*, 2017, vol. 118 (10), pp. 1017–1029. DOI: 10.7868/S0015323017080058. (In Russian).

4. Rogachev A.S. Struktura, stabil'nost' i svoistva vysokoentropiinykh splavov [Structure, stability and properties of high-entropy alloys]. *Fizika metallov i metallovedenie = Physics of Metals and Metallography*, 2020, vol. 121 (8), pp. 807–841. DOI: 10.31857/S0015323020080094. (In Russian).

5. George E.P., Raabe D., Ritchie R.O. High-entropy alloys. *Nature Reviews Materials*, 2019, vol. 4, pp. 515–534. DOI: 10.1038/s41578-019-0121-4.

6. Sharma P., Dwivedi V.K., Dwivedi S.P. Development of high entropy alloys: a review. *Materials Today: Proceedings*, 2021, vol. 43, pp. 502–509. DOI: 10.1016/j.matpr.2020.12.023.

7. Choi W.M., Jo Y.H., Sohn S.S., Lee S., Lee B.J. Understanding the physical metallurgy of the CoCrFeMnNi high-entropy alloy: an atomistic simulation study. *Npj Computational Materials*, 2018, vol. 4 (1), pp. 1–9. DOI: 10.1038/s41524-017-0060-9.

8. Lee C., Maresca F., Feng R., Chou Y., Ungar T., Widom M., An K., Poplawsky J.D., Chou Y.C., Liaw P.K., Curtin W.A. Strength can be controlled by edge dislocations in refractory high-entropy alloys. *Nature Communications*, 2021, vol. 12 (1). DOI: 10.1038/s41467-021-25807-w.

9. Ikeda Y., Grabowski B., Körmann F. Ab initio phase stabilities and mechanical properties of multicomponent alloys: a comprehensive review for high entropy alloys and compositionally complex alloys. *Materials Characterization*, 2019, vol. 147, pp. 464–511. DOI: 10.1016/j.matchar.2018.06.019.

10. Huang T., Jiang H., Lu Y., Wang T., Li T. Effect of Sc and Y addition on the microstructure and properties of HCP-structured high-entropy alloys. *Applied Physics A: Materials Science and Processing*, 2019, vol. 125 (3), pp. 1–5. DOI: 10.1007/s00339-019-2484-1.

11. Santodonato L.J., Liaw P.K., Unocic R.R., Bei H., Morris J.R. Predictive multiphase evolution in Al-containing high-entropy alloys. *Nature Communications*, 2018, vol. 9 (1), pp. 1–10. DOI: 10.1038/s41467-018-06757-2.

12. Wang W.R., Wang W.L., Yeh J.W. Phases, microstructure and mechanical properties of Al_xCoCrFeNi high-entropy alloys at elevated temperatures. *Journal of Alloys and Compounds*, 2014, vol. 589, pp. 143–152. DOI: 10.1016/j.jallcom.2013.11.084.

13. Memon B.A., Yao H. High-pressure induced phase transitions in high-entropy alloys: a review. *Entropy*, 2019, vol. 21 (3). DOI: 10.3390/e21030239.

14. Dong W., Zhou Z., Zhang M., Ma Y., Yu P., Liaw P.K., Li G. Applications of high-pressure technology for high-entropy alloys: a review. *Metals*, 2019, vol. 9 (8), pp. 2–16. DOI: 10.3390/met9080867.

15. Zhou P.F., Xiao D.H., Wu Z., Song M. Microstructure and mechanical properties of AlCoCrFeNi high entropy alloys produced by spark plasma sintering. *Materials Research Express*, 2019, vol. 6 (8). DOI: 10.1088/2053-1591/ab2517.

16. Ivanov I.V., Emurlaev K.I., Ruktuev A.A., Tyurin A.G., Bataev I.A. Struktura vysokoentropiinogo splava AlCoCrFeNi posle deformatsii po skheme odnoosnogo szhatiya i termicheskoi obrabotki [Structure of AlCoCrFeNi high-entropy alloy after uniaxial compression and heat treatment]. *Izvestiya vysshikh uchebnykh zavedenii. Chernaya metallurgiya = Izvestiya. Ferrous Metallurgy*, 2021, vol. 64 (10), pp. 736–746. DOI: 10.17073/0368-0797-2021-10-736-746.

17. Feuerbacher M. Dislocations and deformation microstructure in a B2 ordered $Al_{28}Co_{20}Cr_{11}Fe_{15}Ni_{26}$ high-entropy alloy. *Scientific Reports*, 2016, vol. 6 (1), pp. 1–9. DOI: 10.1038/srep29700.

18. Ma Y., Jiang B., Li C., Wang Q., Dong C., Liaw P.K., Xu F., Sun L. The BCC/B2 morphologies in Al_xNiCoFeCr high-entropy alloys. *Metals*, 2017, vol. 7 (2). DOI: 10.3390/met7020057.

19. Zhu Z., Yang T., Shi R., Quan X., Zhang J., Qiu R., Song B., Liu Q. The effects of annealing at different temperatures on microstructure and mechanical properties of cold-rolled $Al_{0.3}$CoCrFeNi high-entropy alloy. *Metals*, 2021, vol. 11 (6). DOI: 10.3390/met11060940.

20. Rusakov A.A. *Rentgenografiya metallov* [Radiography of metals]. Moscow, Atomizdat Publ., 1977. 479 p.

21. Ivanov I.V., Lazurenko D.V., Stark A., Pyczak F., Thömmes A., Bataev I.A. Application of different diffraction peak profile analysis methods to study the structure evolution of cold-rolled hexagonal α-titanium. *Metals and Materials International*, 2020, vol. 26 (1), pp. 83–93. DOI: 10.1007/s12540-019-00309-z.

Conflicts of Interest

The authors declare no conflict of interest.